Journal of
Materials Chemistry C

This article can be cited before page numbers have been issued, to do this please use: Y. Zhang, Q. Ran, Q. Wang, J. Fan and L. Liao, *J. Mater. Chem. C*, 2019, DOI: 10.1039/C9TC01326A.

ROYAL SOCIETY
OF CHEMISTRY

rsc.li/materials-c

View Article Online
DOI: 10.1039/C9TC01326A

ARTICLE

High-Efficiency Exciplex-Based White Organic Light-Emitting Diodes with a New Tripodal Material as a Co-Host

Received 00th January 20xx,
Accepted 00th January 20xx

DOI: 10.1039/x0xx00000x

Yuan-Lan Zhang,[‡a] Quan Ran,[‡a] Qiang Wang,[a] Jian Fan*[ab] and Liang-Sheng Liao*[ab]

The exciplex-forming co-hosts have been reported to be potentially suitable host for organic light-emitting diodes (OLEDs). However, it might not be able to achieve optimal low voltage and maximal power efficiency (PE), when it comes to white organic light-emitting diodes (WOLEDs). Herein, a novel strategy called multi-exciplex-forming co-hosts (MEHs) is introduced to achieve enhanced efficiency with low operating voltage. To realize this strategy, a new tripodal bipolar compound CNTPA-DPA was synthesized and used as a co-host in the devices. As a result, the orange light-emitting component in the WOLEDs reaches 27% in external quantum efficiency (EQE), 2.1 V in turn-on voltage, and 115.5 lm W^{-1} in PE, which is among the best values of orange color emission in OLEDs. And then this orange light emitting component was adopted in the MEHs strategy to construct WOLEDs, achieving 19.5% of EQE and 73 lm W^{-1} of PE at the maximum, which are 45.7% and 19.6% higher than those of using a single exciplex as the host, respectively. Moreover, the well-matched energy alignment endows the device with a very low operating voltage of 3.8 V at 1000 cd m^{-2}. These results indicate that the performance of the exciplex-based WOLEDs can be remarkably enhanced by using the strategy of MEHs.

1. Introduction

White organic light-emitting diodes (WOLEDs) have attracted close attention as an outstanding candidate for future displays and solid-state lighting sources owing to their superior inherent properties, such as flexibility, light weight, fast response time, and power conservation.[1-4] With the development of hosts and emitters, the performance of WOLEDs has been gradually enhanced to satisfy the demand of real commercialization for cellphones, lamps and televisions.[5] However, achieving high power efficiency (PE) is still a great challenge. At present, the PE of WOLEDs have been achieved beyond 100 lm W^{-1} with outcoupling technology.[6] It should be mentioned that reducing the operating voltage is critically important to improve the PE.[7] Many efforts have been taken in optimizing the performance of WOLEDs, but only a few of them could realize ideal luminance under low driving voltages to achieve high PE. The high voltage issue usually occurs in single-host-based WOLEDs because high carrier injection barrier exists when the wide band gap host materials are used, and the energy loss is hardly avoided between single host and guests in the energy transfer process.[8-10] On the other hand, when using exciplex-forming co-host, the voltage could be lower than that of the conventional single host since the electrons and holes are directly injected to and transported via the lowest unoccupied molecular orbital (LUMO) of acceptors and the highest occupied molecular orbital (HOMO) of donors, respectively.[21] In addition, the exciplex-forming co-host not only maintains effective exciton harvesting from host to dopants but also broadens the recombination zone of excitons which will substantially improve the efficiency and device stability.[11, 12]

However, the situation of WOLEDs is more complicated than that of monochromatic OLEDs, because there are two or more guests doped into the exciplex-forming co-host. In the emitting layer (EML) of the conventional exciplex-based WOLEDs, only single exciplex-forming co-host is usually employed.[13-15, 20] In order to ensure the high triplet (T_1) of exciplex co-host, it requires deep-lying HOMO of electron-donating materials and shallow LUMO of electron-accepting material. As a result, it will create high charge injection barrier between the hole- or electron-transporting layer and the exciplex. In brief, the driving voltage of WOLEDs using single exciplex-forming co-host would result in high voltage.

Here in this work, we aim to further decrease the driving voltage of the exciplex-based WOLEDs. A strategy of multi-exciplex-forming co-hosts (MEHs) was developed in the WOLEDs. In two-color components, the cascade HOMO level alignment of the adjacent exciplex hosts could form "staircases" to remove the hole injection barrier. The triplet energy levels from the lower energy level (for orange emitter) to the higher energy level (for blue emitter) could ensure effective exciton harvesting of different dopants in WOLEDs. As a result, a very low driving voltage of 3.8 V under operating brightness of 1000 cd m^{-2} could be achieved, and both the external quantum efficiency (EQE) and the power efficiency (PE) could be substantially improved.

---

[a] *Institute of Functional Nano & Soft Materials (FUNSOM), Jiangsu Key Laboratory for Carbon-Based Functional Materials & Devices, Soochow University, Suzhou, Jiangsu 215123, China. *E-mail: lsliao@suda.edu.cn; jianfan@suda.edu.cn*

[b] *Institute of Organic Optoelectronics, Jiangsu Industrial Technology Research Institute (JITRI), 1198 Fenhu Avenue, Wujiang, Suzhou, Jiangsu, P. R. China.*

[†] Electronic Supplementary Information (ESI) available. See DOI: 10.1039/x0xx00000x

[‡] These two authors contributed equally to this work.

View Article Online
DOI: 10.1039/C9TC01326A

2. Experimental Details

2.1. Synthesis of New Tripodal Bipolar Compound CNTPA-DPA

Synthesis of 4-(phenylamino)benzonitrile. A mixture of aniline (5.12 g, 55 mmol), 4-bromobenzonitrile (10 g, 55 mmol), tris(dibenzylideneacetone)dipalladium (504 mg 0.55 mmol), 2-Dicyclohexylphosphino-2',6'-dimethoxy-1,1'-biphenyl (452 mg, 1.1 mmol) and sodium tert-butoxide (10.6 g, 110 mmol) in 300 ml of toluene were heated at 80 °C overnight under argon. After cooling down to room temperature, the mixture was extracted with dichloromethane. The combined organic extracts were dried over Na_2SO_4 and evaporated under reduced pressure. The crude product was purified by column chromatography on silica gel using petroleum ether/ dichloromethane (PE/DCM, 8/1, v/v) as the eluent to afford the target compound (8 g, 75 %). ^1H NMR (400 MHz, $CDCl_3$) δ 7.48 (d, J = 8.6 Hz, 2H), 7.36 (t, J = 7.8 Hz, 2H), 7.17 (d, J = 7.8 Hz, 2H), 7.12 (t, J = 7.4 Hz, 1H), 6.97 (d, J = 8.7 Hz, 2H), 6.10 (s, 1H).

Synthesis of 5-chloro-N^1,N^1,N^3,N^3-tetraphenylbenzene-1,3-diamine. A mixture of 1,3-dibromo-5-chlorobenzene (2 g, 7.41 mmol), diphenylamine (2.63 g, 15.56 mmol), tris(dibenzylideneacetone)dipalladium (339 mg, 0.37 mmol), 2-dicyclohexylphosphino-2',6'-dimethoxy-1,1'-biphenyl (457 mg, 1.11 mmol) and sodium tert-butoxide (2.85 g, 29.64 mmol) in 100 ml of toluene were heated at 80 °C for 4 hours under argon. After cooling down to room temperature, the mixture was extracted with dichloromethane. The combined organic extracts were dried over Na_2SO_4 and evaporated under reduced pressure. The crude product was purified by column chromatography on silica gel using petroleum ether/dichloromethane (PE/DCM, 4/1, v/v) as the eluent to afford the target compound with a yield of 50%. ^1H NMR (400 MHz, $CDCl_3$) δ 7.22 (t, J=7.8 Hz, 8H), 7.06 (d, J=7.8 Hz, 8H), 7.00 (t, J=7.3 Hz, 4H), 6.65 (s, 1H), 6.56 (d, J=1.8 Hz, 2H).

Synthesis of CNTPA-DPA. A mixture of 5-chloro-N^1,N^1,N^3,N^3-tetraphenylbenzene-1,3-diamine (1.05 g, 2.36 mmol), 4-(phenylamino)benzonitrile (551 mg, 2.84 mmol), tris(dibenzylideneacetone)dipalladium (109 mg, 0.12 mmol), tri-*t*-butylphosphonium tetrafluoroborate (104 mg, 0.36 mmol) and sodium tert-butoxide (910 mg, 9.48 mmol) in 100 ml of toluene were heated at 110 °C overnight under nitrogen. After cooling down to room temperature, the mixture was extracted with dichloromethane. The combined organic extracts were dried over Na_2SO_4 and evaporated under reduced pressure. The crude product was purified by column chromatography on silica gel using petroleum ether/ dichloromethane (PE/DCM, 1/1, v/v) as the eluent to afford a white solid (717 mg, 68 %). ^1H NMR (400 MHz, DMSO-d_6) δ 7.56 (d, J=8.7 Hz, 2H), 7.34 (t, J=7.7 Hz, 2H), 7.23 (t, J=7.8 Hz, 8H), 7.13 (dd, J=7.7 Hz, 3H), 7.05 – 6.91 (m, 14H), 6.29 (s, 1H), 6.23 – 6.14 (m, 2H). ^{13}C NMR (151 MHz, $CDCl_3$) δ 151.03, 149.43, 147.07, 146.93, 145.39, 132.95, 129.60, 129.10, 125.99, 125.07, 124.17, 123.04, 119.80, 119.47, 115.04, 114.89, 102.21. MALDI-TOF-MS: m/z: calcd for $C_{43}H_{32}N_4$: 604.76, found: 604.19. The complexes were fully characterized by ^1H and ^{13}C NMR (Fig. S1-S4, ESI†) and MALDI-TOF mass spectrometry.

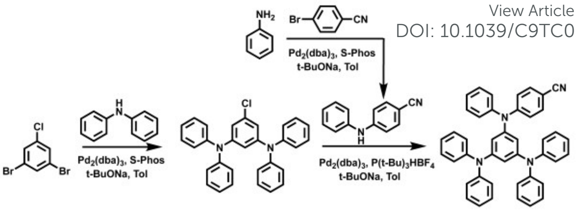

Scheme 1 The synthetic route of CNTPA-DPA.

2.2. OLED Fabrication and Measurements

The OLEDs were fabricated through vacuum deposition under vacuum of 4×10^{-6} Torr and on commercially pre-patterned ITO-coated glass substrates (32 mm×32 mm×0.7 mm) with the ITO thickness of 135 nm and a sheet resistance of 15 Ω per square. The emitting area of each device is 0.09 cm^2. The ITO substrates were ultrasonically cleaned with acetone and ethanol for 15 min subsequently, and then dried in an oven at 110 °C for 1 h and finally treated by UV-ozone for 15 min. The deposition rate was controlled at 0.3-0.4 Å/s for 1,4,5,8,9,11-hexaazatriphenylenehexacarbonitrile (HAT-CN), 0.2-0.4 Å/s for 8-hydroxyquinolatolithium (Liq), 1-2 Å/s for other organic layers and 6-8 Å/s for Al anode. The Electroluminescence (EL) spectra, efficiencies, Commission Internationale de L'Eclairage (CIE) coordinates, current density-voltage-luminance curves, current efficiencies and power efficiencies of the OLEDs were measured with a programable spectra scan photometer (PHOTO RESEARCH, PR 655) and a constant current source meter (KEITHLEY 2400) at room temperature.

3. Results and Discussion

3.1. Material Properties

CNTPA-DPA has a tripodal structure, and three functional groups are attached to 1,3,5-positions of the central benzene ring, which are shown in Fig. 1a. In this novel bipolar compound, diphenylamine (DPA) and benzonitrile are applied as electron-donating and electron-withdrawing groups, respectively, offering independent channels for hole and electron transport. The density functional theory (DFT) calculations were also carried out. As shown in Fig. 1b, the HOMOs of the material are mainly located on the DPA units, while the LUMOs are mainly distributed on the benzonitrile and the central benzene motif. The UV-Vis absorption and photoluminescence (PL) spectra of CNTPA-DPA were also collected to study the photophysical properties as shown in Fig. 1c. The strong structureless absorption for CNTPA-DPA at approximately 305 nm could be corresponding to the π-π* absorption from the backbone. Estimated from the peaks of fluorescence and phosphorescence spectra, the S_1 and T_1 energies were about 3.01 and 2.74 eV, respectively. Besides, Cyclic voltammetry (CV) was carried out at room temperature to estimate the HOMO energy level of CNTPA-DPA and the calculated result was about -5.76 eV (Fig. S5, ESI†). Given the difference of HOMO and LUMO energy level is nearly about the value of the corresponding optical bandgap, the LUMO could also be calculated to be -2.49 eV. Moreover, thermogravimetric analysis (TGA) and differential scanning

View Article Online
DOI: 10.1039/C9TC01326A

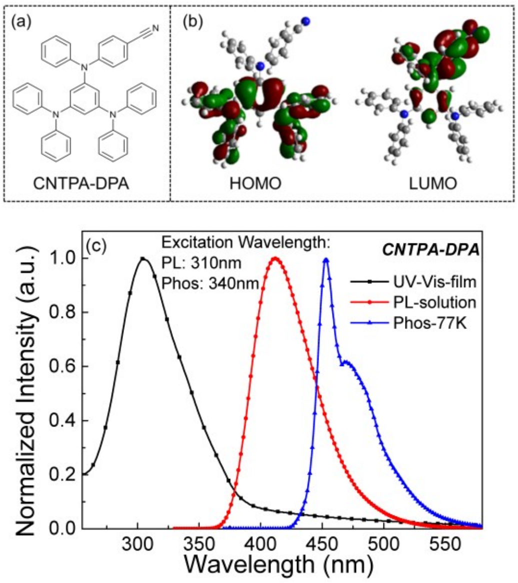

Fig. 1 (a) Molecular structures of CNTPA-DPA. (b) Frontier molecular orbitals distribution of CNTPA-DPA. (c) UV-Vis absorption, fluorescence (300 K), and phosphorescence (77 K) spectra of CNTPA-DPA.

calorimetry (DSC) measurements have been tested as shown in Fig. S6 (ESI†). Hole-only devices of CNTPA-DPA and 1,3-bis(N-carbazolyl)benzene (mCP) were also fabricated to compare their hole-injection (Fig. S7, ESI†). The hole current densities of CNTPA-DPA is much higher than that of mCP, indicating a better hole-injection, which will contribute to enhance the device efficiency. Based on the space-charge-limited-current (SCLC) model, the hole mobility of CNTPA-DPA was calculated to be 7.8×10^{-8} cm^2 V^{-1} s^{-1}. All physical properties of CNTPA-DPA were summarized in Table S1 (ESI†).

3.2. Photophysical & Electroluminescent Properties

We employed CNTPA-DPA as the donor to form a new exciplex-forming co-host with a conventional acceptor (1,3,5-triazine-2,4,6-triyl)tris(benzene-3,1-diyl)tris-(diphenylphosphineoxide) (PO-T2T). The molecular structures of mCP and PO-T2T are shown in Fig. 2a, respectively. The PL spectra of the material CNTPA-DPA, mCP, PO-T2T, CNTPA-DPA co-deposited with PO-T2T film and mCP co-deposited with PO-T2T film are shown in Fig. 2b. Since CNTPA-DPA and PO-T2T have an emission peak at 426 nm and 395 nm, respectively, the CNTPA-DPA: PO-T2T mixed film showed a feature-less broad emission, peaked at 535 nm and a bathochromic shift compared with either CNTPA-DPA or PO-T2T. It indicated an intermolecular D-A interaction and the successful formation of new exciplex. In order to calculate the T_1 energy of CNTPA-DPA: PO-T2T, we tested the phosphorescence spectra at 77K as shown in Fig. S11. From the peak of the phosphorescence spectra, the triplet energy of CNTPA-DPA: PO-T2T was determined to be 2.32 eV. The PL lifetime spectra of CNTPA-DPA: PO-T2T mixed film in Fig. 2c further proved this phenomenon, including a fast decay component of 61.3 ns and a much slower decay with lifetime longer than 4.2 μs. The PL spectra and PL lifetime spectra of co-deposited mCP: PO-T2T mixed film also indicated the succeed of exciplex.

Simplified device structures doped with orange phosphor Iridium(III) bis(4-phenylthieno[3,2-c]pyridinato-N, C2′) (PO-01) based on this new exciplex-forming co-host were designed, which was established as ITO/HAT-CN (10 nm)/TAPC (40 nm)/TCTA (10 nm)/CNTPA-DPA: PO-T2T: PO-01 (1:1 6 wt%, 20 nm)/PO-T2T (50 nm)/Liq (2 nm)/Al (120 nm). Fig. 3a shows the device structure and energy-level diagram. Here, HAT-CN and Liq are the hole- and electron-injecting layer. Di[4-(*N*,*N*-ditolyl-amino)-phenyl]cyclohexane (TAPC) and tris(4-(9Hcarbazol-9-yl)phenyl)amine (TCTA) act as the hole-transporting layers. PO-T2T is the electron transporting layer. PO-01 is the dopant as guest. The device structure of orange phosphorescent organic light-emitting diodes was well optimized and the turn-on voltage was as low as 2.1 V. A high maximum power efficiency of 115.5 lm W^{-1} and maximum EQE of 27% were achieved, which is among the highest values to our knowledge.[16-17, 19] The high efficiency of this orange OLEDs indicated that excitons generated from the exciplex-forming co-host could be efficiently harvested by PO-01 in the emitting-layer.

In traditional exciplex-based WOLEDs structure, the donor of exciplex-forming co-host must have a high T_1 to block the generated excitons for the harvesting in the EML and should has a deep HOMO to form exciplex-forming co-host with acceptor for the effective energy transfer to all the dopants, especially the blue one. The conventional exciplex system cannot avoid the energy loss from exciplex-forming co-host to different dopants. For instance, because the orange phosphor PO-01 has a narrow energy band gap, the excitons generated by the holes on HOMOs of mCP and the electrons on the LUMOs of PO-T2T will have excessive energy for it and there must be energy loss in the transfer. In addition, the sharp change in HOMO between TCTA and mCP severely hinder the hole injection, which will

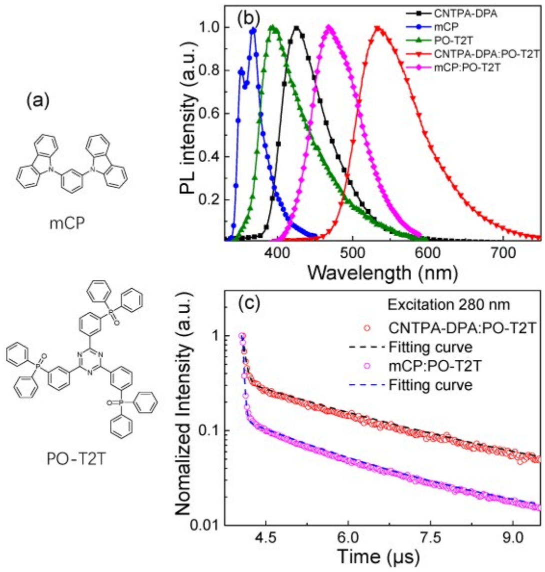

Fig. 2 (a) Molecular structures of mCP and PO-T2T. (b) PL spectra of CNTPA-DPA, mCP, PO-T2T, CNTPA-DPA:POT2T, mCP:PO-T2T, all of solid films were measured at 280 nm excitation. (c) Transient PL decay curve of CNTPA-DPA:PO-T2T, mCP:PO-T2T co-doped film (measured at 300K).

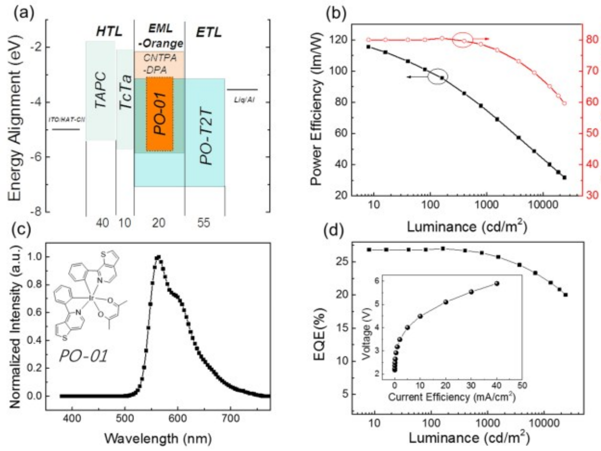

Fig. 3 EL characteristics of the orange OLEDs. (a) Schematic diagram of the device structure and energy level. (b) PE-*L*-CE curve. (c) EL spectral at 5 mA/cm^2. (d) EQE-*L* curve.

bring the charge injection barrier and high driving voltage. CNTPA-DPA has a high T_1 (2.74 eV) to block the generated excitons and its suitable HOMO (-5.76 eV) would provide a "staircase" for the hole-injection/transport from TCTA to mCP, which decrease the carrier injection barrier. More importantly, it has quite high hole mobility than mCP, indicating better hole injection/transport to further improve the efficiency. What's more, CNTPA-DPA and PO-T2T successfully form an effective exciplex as host of PO-01, which was confirmed in the former part.

To explore its possibility of utility value in WOLEDs, we designed and fabricated white devices by utilizing the MEHs strategy. mCP and PO-T2T could successfully form exciplex as host of a blue phosphor Iridium(III)[bis(4,6-difluorophenyl)-pyridinato-N,C2′] picolinate (FIrpic).[18] In traditional structure of exciplex-based WOLEDs, this exciplex could be used as the host of blue and orange emitters because mCP and PO-T2T both have highly enough T1 to block the excitons for effective harvesting. But the high energy level of T1 also brings the high voltage. To solve this problem and further improve the performance, we employed the strategy of MEHs, The optimized device structure was fabricated as following (W1, shown in Fig. 4a): ITO/HAT-CN (10 nm)/TAPC (40 nm)/TCTA (10 nm)/CNTPA-DPA: PO-T2T: PO-01 (1:1 4 wt%, 3 nm)/mCP: PO-T2T: FIrpic (1:1 15 wt%, 20 nm)/PO-T2T (45 nm)/Liq (2 nm)/Al (120 nm). For comparison with traditional exciplex-based WOLEDs, W2 was fabricated as following: ITO/HAT-CN (10 nm)/TAPC (40 nm)/TCTA (10 nm)/mCP: PO-T2T: PO-01 (1:1 4 wt%, 3 nm)/mCP: PO-T2T: FIrpic (1:1 15 wt%, 20 nm)/PO-T2T (45 nm)/Liq (2 nm)/Al (120 nm). In the multi-EML, the white emission composed of orange emission and blue emission. The difference of these two WOLEDs focused on the orange part. In reference device W2, the orange dopant simply adopted the same exciplex-forming co-host as the blue part, which will result in high voltage and energy loss. While in W1, blue and orange dopant were allocated to distinct exciplex-forming co-hosts, and the one for orange dopants was more efficient and could avoid the energy loss in the energy transfer. The schematic diagram of the energy transfer routes of MEHs system is shown in Fig. S10. Owing to the well-matched HOMO level alignment between TCTA, CNTPA-DPA and mCP, the hole-injection/transport is enhanced compared to W2. Besides, the hole mobility of CNTPA-DPA is faster than mCP, which will further enhance the efficiency. Benefited from CNTPA-DPA and MEHs strategy, a remarkable enhancement of efficiency could be achieved. W1 achieved an enhancement of PE by 45.7% and EQE by 19.6% at the maximum in contrast to W2. Besides, the well-matched energy alignment endows the device W1 with a very low operating voltage of 3.8V at 1000 cd m^{-2}, which is decreased by 0.3 V in comparison with W2. In addition, W1 exhibits slightly cooler white-emission with correlated color temperature (CCT) ≈ 4000 K contrast to 3500 K of W2 and the CIE coordinates were optimized from (0.44, 0.48) to (0.41, 0.48), this enhancement may due to the better hole-injection and transport in the EML. It should be noted that the CIE coordinates shift from (0.46, 0.50) to (0.34, 0.46) with driving voltage varying from 3 V to 6 V in W1, which might be due to the increasing exciton harvesting in the blue part of the multi-EML. To further investigate the effect of the intermediate HOMO level of CNTPA-DPA in the MEHs strategy, we exchanged the sequence of blue emitting layer and orange emitting layer and fabricated W3 with a configuration of ITO/HAT-CN (10 nm)/TAPC (40 nm)/TCTA (10 nm)/ mCP: PO-T2T: FIrpic (1:1 15 wt%, 20 nm)/CNTPA-DPA: PO-T2T: PO-01 (1:1 4 wt%, 3 nm)/PO-T2T (45 nm)/Liq (2 nm)/Al (120 nm) (Fig. S8, ESI†). Impressively, W3 exhibits higher color stability with a slight shift in the CIE coordinated ΔCIE = (0.02, 0.00) from (0.40, 0.47) at 1000 cd m^{-2} to (0.38, 0.47) at 8000 cd m^{-2}. In addition, benefited from the MEHs strategy, W3 also shows high performance with a maximum EQE of 16.8%. At 1000 cd m^{-2}, there was a negligible decrease for EQE of 16.5%, with a roll-off

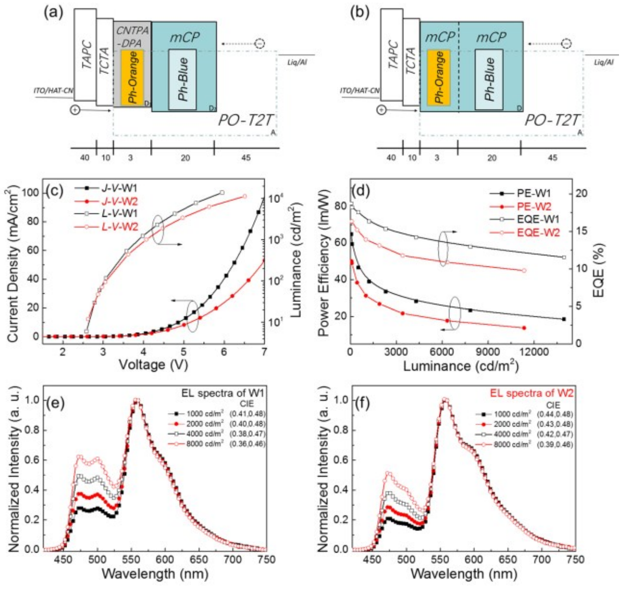

Fig. 4 EL characteristics of W1, W2. (a, b) Schematic diagram of the device structure W1, W2. (c) Current Density-Voltage-Luminance (*J*-*V*-*L*) curves of W1, W2. (d) PE-Luminance-EQE (PE-*L*-EQE) curves of W1, W2. (e, f) Normalized EL spectra at various luminance of 1000, 2000, 4000 and 8000 cd m^{-2} and the corresponding CIE values of W1, W2.

View Article Online
DOI: 10.1039/C9TC01326A

Table 1 EL Performance of Three Different WOLEDs.

Devices	Voltage		Maximum/at 1000 cd m^{-2}			CIE^c (x,y)
	(V)^a	(V)^b	PE (lm W^{-1})	CE (cd A^{-1})	EQE (%)	
W1	2.4	3.8	73/41.9	60/49.5	19.5/16	(0.41,0.48)
W2	2.5	4.1	50.1/31.2	47.5/40.4	16.3/13.9	(0.44,0.48)
W3	2.8	4.9	40.6/32.7	49.3/48.5	16.8/16.5	(0.40,0.47)

[a,b] Voltages were measured corresponding to onset and 1000 cd m^{-2}, respectively.
[c] Commission International de I'Eclairage (CIE) coordinates tested at 1000 cd m^{-2}.

of just 1.8%. Unfortunately, owing to the sharp change in HOMO between TCTA and mCP, W3 shows higher turn-on voltage and driving voltage than W1, which represents the critical effect of the suitable energy level matches. Moreover, we also fabricated W4 based on single exciplex-forming co-host composed of CNTPA-DPA and PO-T2T. As shown in Fig. S9 (ESI†), the device W4 was fabricated as ITO/HAT-CN (10 nm)/TAPC (40 nm)/TCTA (10 nm)/CNTPA-DPA: PO-T2T: FIrpic (1:1 15 wt%, 20 nm)/CNTPA-DPA: PO-T2T: PO-01 (1:1 4 wt%, 3 nm)/PO-T2T (45 nm)/Liq (2 nm)/Al (120 nm). Unfortunately, due to the low triplet energy (2.32 eV) of the exciplex-forming co-host (CNTPA-DPA: PO-T2T), the device W4 exhibits only orange emission with negligible blue component. All the performance of the white devices was summarized in Table 1. To sum up, the maximum PEs and EQEs of W1, W2 and W3 were 73 lm W^{-1}, 47.5 lm W^{-1}, 49.3 lm W^{-1} and 19.5%, 16.3%, 16.8%, respectively. At 1000 cd m^{-2}, the PEs and EQEs could maintain levels as 41.9 lm W^{-1}, 31.2 lm W^{-1}, 32.7 lm W^{-1} and 16%, 13.9%, 16.5%, respectively, with a slight efficiency roll-off. Device W1 achieved a very low operating voltage of about 3.8 V at 1000 cd m^{-2}, while 4.1 V for Device W2 and 4.9 V for Device W3. These results confirmed the superiority for utilizing the strategy of MEHs in exciplex-based WOLEDs.

4. Conclusions

In conclusion, a new tripodal bipolar compound CNTPA-DPA was synthesized and employed to assist this strategy of multi-exciplex-forming co-hosts (MEHs) in exciplex-based WOLEDs. Benefited from the valuable properties of CNTPA-DPA, especially the high hole mobility and suitable HOMO, the orange color emitting component for the WOLEDs could reach 27% in external quantum efficiency (EQE), 2.1 V in turn-on voltage, and 115.5 lm W^{-1} in power efficiency, which is believed among the best values of orange color emission in OLEDs. By utilizing the strategy of MEHs, we alleviate the problem of high voltage and energy loss in traditional WOLEDs using single exciplex-forming co-host. As a result, we realize considerable enhancement in efficiency and decrease in operating voltage. The optimized WOLEDs showed enhancement of PE by 45.7% and EQE by 19.6% at the maximum in contrast to the traditional single exciplex-based WOLEDs. Particularly, the well-matched energy alignment endows the device with a very low operating voltage of 3.8 V at 1000 cd m^{-2}, which is decreased by 0.3 V. These results showed obvious improvement of performance in WOLEDs and the effective strategy of MEHs offered a new option for WOLEDs structure characteristics and showed another way to design materials for exciplex-employing in high-performance WOLEDs.

Conflicts of interest

The authors declare no competing financial interest.

Acknowledgements

The authors acknowledge the financial support from the National Natural Science Foundation of China (51821002, 61575136) and the National Key R&D Program of China (2016YFB0400700). This work was also funded by the Collaborative Innovation Centre of Suzhou Nano Science and Technology (Nano-CIC), Priority Academic Program Development of Jiangsu Higher Education Institutions (PAPD), and "111" Project of The State Administration of Foreign Experts Affairs of China.

References

1 B. W. D'Andrade and S. R. Forrest, *Advanced Materials*, 2004, **16**, 1585-1595.
2 Y. Sun, N. C. Giebink, H. Kanno, B. Ma, M. E. Thompson and S. R. Forrest, *Nature*, 2006, **440**, 908-912.
3 H. Uoyama, K. Goushi, K. Shizu, H. Nomura and C. Adachi, *Nature*, 2012, **492**, 234-238.
4 C. W. Tang and S. A. VanSlyke, *Applied Physics Letters*, 1987, **51**, 913-915.
5 H. Sasabe and J. Kido, *Journal of Materials Chemistry C*, 2013, **1**, 1699.
6 K. Udagawa, H. Sasabe, F. Igarashi and J. Kido, *Advanced Optical Materials*, 2016, **4**, 86-90.
7 H. Sasabe, H. Nakanishi, Y. Watanabe, S. Yano, M. Hirasawa, Y.-J. Pu and J. Kido, *Advanced Functional Materials*, 2013, **23**, 5550-5555.
8 X. Tang, X. Y. Liu, Y. Yuan, Y. J. Wang, H. C. Li, Z. Q. Jiang and L. S. Liao, *ACS applied materials & interfaces*, 2018, **10**, 29840-29847.
9 E. Mondal, W.-Y. Hung, H.-C. Dai and K.-T. Wong, *Advanced Functional Materials*, 2013, **23**, 3096-3105.
10 A. Chaskar, H. F. Chen and K. T. Wong, *Adv Mater*, 2011, **23**, 3876-3895.
11 P. Xiao, J. Huang, Y. Yu, J. Yuan, D. Luo, B. Liu and D. Liang, *Applied Sciences*, 2018, **8**, 1449.
12 Y.-S. Park, S. Lee, K.-H. Kim, S.-Y. Kim, J.-H. Lee and J.-J. Kim, *Advanced Functional Materials*, 2013, **23**, 4914-4920.
13 Z. Chen, X.-K. Liu, C.-J. Zheng, J. Ye, C.-L. Liu, F. Li, X.-M. Ou, C.-S. Lee and X.-H. Zhang, *Chemistry of Materials*, 2015, **27**, 5206-5211.
14 X. K. Liu, Z. Chen, J. Qing, W. J. Zhang, B. Wu, H. L. Tam, F. Zhu, X. H. Zhang and C. S. Lee, *Advanced Materials*, 2015, **27**, 7079-7085.
15 N. Sun, Q. Wang, Y. Zhao, Y. Chen, D. Yang, F. Zhao, J. Chen and D. Ma, *Adv Mater*, 2014, **26**, 1617-1621.
16 S. Lee, K. H. Kim, D. Limbach, Y. S. Park and J. J. Kim, *Advanced Functional Materials*, 2013, **23**, 4105-4110.
17 R. Wang, D. Liu, H. Ren, T. Zhang, H. Yin, G. Liu and J. Li, *Adv Mater*, 2011, **23**, 2823-2827.
18 J.-H. Lee, S.-H. Cheng, S.-J. Yoo, H. Shin, J.-H. Chang, C.-I. Wu, K.-T. Wong and J.-J. Kim, *Advanced Functional Materials*, 2015, **25**, 361-366.
19 T. Xu, Y. X. Zhang, B. Wang, C. C. Huang, I. Murtaza, H. Meng and L. S. Liao, ACS Appl. Mater. Interfaces, 2017, 9, 2701-2710.
20 T. Xu, J.-G. Zhou, M.-K. Fung and H. Meng, Organic Electronics, 2018, 63, 369-375.

View Article Online
DOI: 10.1039/C9TC01326A

21 T. Xu, J. G. Zhou, C. C. Huang, L. Zhang, M. K. Fung, I. Murtaza, H. Meng and L. S. Liao, ACS Appl. Mater. Interfaces, 2017, 9, 10955-10962.

View Article Online
DOI: 10.1039/C9TC01326A

Table of Contents Graphic

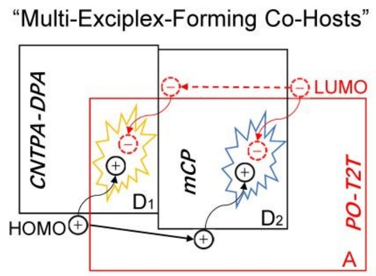

An evident enhancement of performance in exciplex-based WOLEDs utilizing the effective strategy of multi-exciplex-forming co-hosts (MEHs) was achieved.